ARL-TR-7526 ● Nov 2015

US Army Research Laboratory

Characterization of Sputtered Nickel-Titanium (NiTi) Stress and Thermally Actuated Cantilever Bimorphs Based on NiTi Shape Memory Alloy (SMA)

by Merric D Srour, Cory R Knick, and Christopher J Morris

NOTICES

Disclaimers

The findings in this report are not to be construed as an official Department of the Army position unless so designated by other authorized documents.

Citation of manufacturer's or trade names does not constitute an official endorsement or approval of the use thereof.

Destroy this report when it is no longer needed. Do not return it to the originator.

ARL-TR-7526 ● Nov 2015

US Army Research Laboratory

Characterization of Sputtered Nickel-Titanium (NiTi) Stress and Thermally Actuated Cantilever Bimorphs Based on NiTi Shape Memory Alloy (SMA)

by Merric D Srour, Cory R Knick, and Christopher J Morris
Sensors and Electron Devices Directorate, ARL

REPORT DOCUMENTATION PAGE

Form Approved
OMB No. 0704-0188

1. REPORT DATE *(DD-MM-YYYY)*	2. REPORT TYPE	3. DATES COVERED (From - To)
November 2015	Final	05/2015 to 10/2015

4. TITLE AND SUBTITLE
Characterization of Sputtered Nickel-Titanium (NiTi) Stress and Thermally Actuated Cantilever Bimorphs Based on NiTi Shape Memory Alloy (SMA)

5a. CONTRACT NUMBER

5b. GRANT NUMBER

5c. PROGRAM ELEMENT NUMBER

6. AUTHOR(S)
Merric D Srour, Cory R Knick, and Christopher J Morris

5d. PROJECT NUMBER

5e. TASK NUMBER

5f. WORK UNIT NUMBER

7. PERFORMING ORGANIZATION NAME(S) AND ADDRESS(ES)
U.S. Army Research Laboratory
ATTN: RDRL-SER-L
2800 Powder Mill Road
Adelphi, MD 20783-1138

8. PERFORMING ORGANIZATION REPORT NUMBER
ARL-TR-7526

9. SPONSORING/MONITORING AGENCY NAME(S) AND ADDRESS(ES)

10. SPONSOR/MONITOR'S ACRONYM(S)

11. SPONSOR/MONITOR'S REPORT NUMBER(S)

12. DISTRIBUTION/AVAILABILITY STATEMENT
Approved for public release; distribution is unlimited.

13. SUPPLEMENTARY NOTES

14. ABSTRACT
Nickel-titanium (NiTi) based thin films are the most commonly used material for shape memory alloys (SMAs). We report on our NiTi sputter process and results for fabricating thin-film NiTi microelectromechanical system (MEMS) cantilevers. To produce a repeatable and optimal process for depositing NiTi thin films, we focused on varying the sputter parameters during NiTi deposition, such as thickness, substrate temperature during deposition and anneal, and argon pressure during deposition. We recorded equilibrium heating and cooling videos of released NiTi cantilevers, which were used to study the cantilever bending as a function of temperature. We determined that on heating, the cantilevers gradually curled upward from 30 to 74 °C, at which point they rapidly folded flat. On cooling, the cantilevers rapidly curled at 63 °C and remained curled until 40 °C, at which point they gradually flattened as cooled to room temperature. We measured stress as a function of temperature for NiTi on silicon (Si), obtaining room temperature residual stresses as low as –29 MPa. In addition, we achieved a residual stress differential of up to 882 MPa, corresponding to useful actuation. Further research is needed to optimize the film properties and produce a consistent process for achieving low residual stress MEMS cantilevers.

15. SUBJECT TERMS
MEMS, shape memory alloy, thermal actuation, process development, residual stress

16. SECURITY CLASSIFICATION OF:			17. LIMITATION OF ABSTRACT	18. NUMBER OF PAGES	19a. NAME OF RESPONSIBLE PERSON
a. REPORT	b. ABSTRACT	c. THIS PAGE			Cory R Knick
Unclassified	Unclassified	Unclassified	UU	28	19b. TELEPHONE NUMBER (Include area code) 301-394-1147

Standard Form 298 (Rev. 8/98)
Prescribed by ANSI Std. Z39.18

Contents

List of Figures

List of Tables

Acknowledgments

We wish to acknowledge Brian Isaacson for fabrication of devices in the Cleanroom and Sam Hirsh at Aberdeen Proving Ground for the energy-dispersive x-ray (EDX) measurements.

INTENTIONALLY LEFT BLANK.

1. Introduction

Thin-film shape memory alloy (SMA) is a promising material for microelectromechanical system (MEMS) actuators. This is because it delivers a large output force per unit volume, works as both a functional and structural element, can be actuated electrically or thermally, and shows both thermal and mechanical shape memory.[1–4] Out of the many different potential SMAs, nickel-titanium (NiTi) and nickel-titanium-copper (NiTiCu) based alloys have been proven as being both commercially practical and having useful engineering properties.[3] However, since Cu-based alloys are brittle in polycrystalline states, most MEMS applications focus on using NiTi-based alloys.[2] NiTi thin films for MEMS applications compared to other actuation mechanisms such as thermal, magnetic, or electrostatic are more useful because of their high power density, actuation force, and large displacement, and high work output per volume.[1,5]

The basic phenomenon of the shape memory effect is the phase transition between a low temperature, low symmetry martensite phase and the relatively high temperature, high symmetry austenite phase, which is a reversible process.[6] During heating, a significant increase in stress is present due to the change from martensite to austenite.[7] Figure 1 shows the martensite and austenite cubic structures (left) and a schematic plot depicting the phase transformation from lower temperature martensite to higher temperature austenite and the reverse transformation through an arbitrary heating and cooling cycle (right).[16] A_s, A_f, M_s, and M_f represent the austenite start, austenite finish, martensite start, and martensite finish temperatures, respectively.

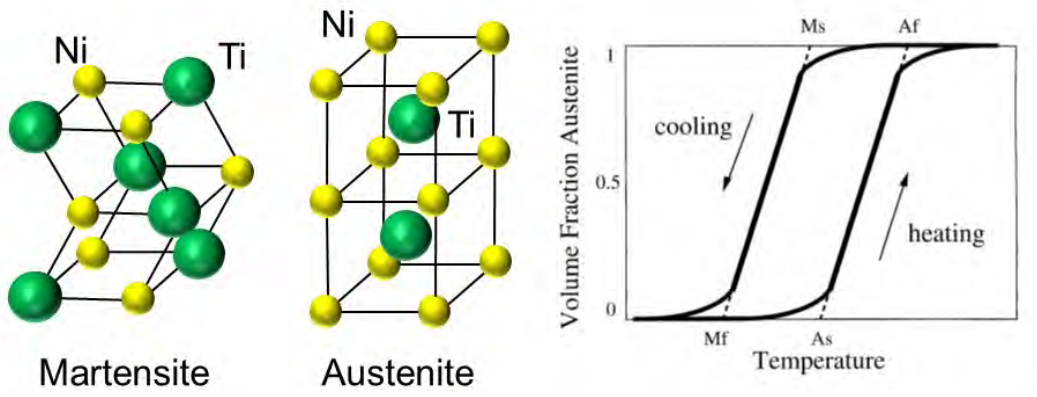

Fig. 1 Cubic structure of the martensite and austenite phases in NiTi alloy and a schematic diagram showing the phase transformation of low temperature martensite to higher temperature austenite phase in NiTi[16]

In order to achieve the shape memory effect from the thin-film NiTi alloy above room temperature, it is very important that the NiTi composition be equiatomic.[1] A small change of even 1 atomic percent (at. %) near the equiatomic composition can shift the phase change by as much as 100 °C.[6] Therefore, the NiTi composition is generally targeted at $Ni_{50}Ti_{50}$.

NiTi thin films have been developed using many different techniques such as DC magnetron sputtering, radio frequency (RF) magnetron sputtering, ion beam sputtering, laser ablation, and flash evaporation.[8] However, it has been well established that sputter deposition is the most practical technique for depositing NiTi with sufficient shape memory effect.[6,9–15] Sputtering is the best option for depositing NiTi thin films because the conventional vacuum evaporation of NiTi leads to the potential problem of difference in evaporation rate due to difference in vapor pressure, thus making composition control more difficult.[1] One of the techniques used for sputtering NiTi onto silicon (Si) wafers is simultaneous co-sputtering from a $Ni_{50}Ti_{50}$ alloy and pure Ti targets. It was noted quite early that the composition of sputtered films from a NiTi target does not match the composition of the target, but rather ends up being Ti deficient. Therefore, a second pure Ti target is commonly added to enable precise composition control of the resulting thin film.[6,16]

Previously, we developed a co-sputtered NiTi thin-film material deposition process and characterized the material.[17] We also developed a fabrication process to enable free-standing NiTi/platinum (Pt) cantilever thermal actuators and demonstrated their basic operation.[18,19] In this report, we demonstrate an improved material with greater than 5 times higher recovery stress and more thoroughly characterize the mechanical behavior through film stress measurements as a function of temperature as well as observations of the temperature-dependent curvature of released structures. Large recovery stress is generally preferred for actuation in MEMS applications[7] so a natural focus was to achieve large recovery stresses in films as thin as possible. By varying the sputtering parameters of NiTi such as temperature of the wafer during deposition and anneal, argon (Ar) pressure during sputtering, and NiTi thickness, we achieved a more optimal process for producing NiTi cantilevers with an actuation temperature near 60 °C. Our study reveals that we can achieve sufficient shape recovery properties in NiTi films as thin as 270 nm. In our future studies, we intend to test devices of reduced NiTi thickness compared to those here.

2. Methods

2.1 Co-Sputtering of NiTi

The equiatomic NiTi films were co-sputtered using an AJA ATC 2200 co-sputter tool with independent DC power supplies to 2 separate 4-inch targets. We used a $Ni_{50}Ti_{50}$ target with 375 W of DC power and a pure Ti target with 300 W DC power for a simultaneous co-sputter process. Substrate rotation was used during sputtering to obtain optimal uniformity and Ar pressures of 2, 5, and 10 mTorr were tested as deposition parameters. We sputter-deposited various thicknesses from 250 to 1500 nm at the 3 different Ar pressures to ascertain the effect of multiple parameters for the co-sputtering process.

The films were characterized using multiple techniques including electrical resistivity measurements on a 280SI Sheet 4-point Resistivity Measurement System used to quantify film uniformity across a 4-inch wafer. Additionally, we performed energy-dispersive x-ray (EDX) film composition analysis using a Hitachi S-4500 scanning electron microscope (SEM) equipped with a PRISM^{60} Princeton Gamma Tech detector using a beam acceleration voltage of 20 kV.

2.2 Stress vs. Temperature Measurements

Stress versus temperature measurements were performed using a Toho FLX-2320-S wafer bow tool with controlled heating and cooling from room temperature (RT) to 100 °C with a heating and cooling rate of 3 °C/min. For these experiments, we prepared films of NiTi by sputtering onto 4-inch Si wafers at 600 °C in order to crystallize the material during sputtering. Wafer bow was measured experimentally from RT to 100 °C at 3 °C/min heating/cooling rate, which allowed us to calculate and plot the temperature-dependent residual stress in the NiTi film for each wafer sample. We calculated the residual stress in the NiTi thin film based on Stoney's equation, which is given as

$$\sigma = \frac{E}{6(1-\nu)} \frac{{h_s}^2}{h} \left(\frac{1}{R} - \frac{1}{R_0} \right) \quad (1)$$

Here, σ is the stress in the thin film; and E, ν, and h_s are Young's modulus of Si, Poisson ratio of the Si substrate, and the thickness of the Si substrate, respectively. The variable h represents the thin-film thickness, while R and R_0 represent the radii of curvature of the film-Si substrate composite and the curvature of the bare Si substrate prior to film deposition, respectively.

$$\sigma_{NiTi} = \frac{E\, {h_s}^2}{6(1-\nu)h_{NiTi}}\left(\frac{1}{R} - \frac{1}{R_0} - \left(\frac{6(1-\nu)}{E}\right)\left(\frac{\sigma_{Pt}(h_{NiTi+Pt} - h_{NiTi})}{{h_s}^2}\right)\right) \quad (2)$$

We used an extended version of Stoney's equation, as shown above, in order to calculate the stress in the NiTi when NiTi was deposited on a layer of Pt. σ_{NiTi} is the stress in the NiTi layer; E, ν, and h_s are Young's modulus of Si, Poisson ration of the Si substrate, and the thickness of the Si substrate, respectively; and σ_{Pt} represents the stress in the annealed Pt. The variable h_{NiTi} represents the NiTi thin-film thickness, and R and R_0 represent the radius of curvature of the NiTi film/annealed Pt/Si substrate composite and the initial radius curvature of the Si substrate, respectively.

2.3 Cantilever Fabrication and Dry Etch Release Method

Our wafer frontside dry-etch release process is depicted in Fig. 2. Starting with a 4-inch Si wafer with a 170-nm Pt backside layer and a 200-nm silicon nitride (Si_3N_4) frontside layer, we etched lithographically patterned regions of Si_3N_4 down to the Si substrate. Following this, we liftoff patterned a thermally evaporated 200-nm Pt layer with a 10-nm chromium (Cr) adhesion layer to create a differential stress distribution across each cantilever when combined with the SMA. Pt was selected to withstand the 600 °C anneal required to crystallize NiTi, after we demonstrated that gold (Au) could not survive the necessary anneal. Following this, a thin film of NiTi was blanket sputtered at 600 °C. This NiTi blanket layer was then wet-etch patterned using a 2:2:20 solution of hydrogen fluoride (HF), nitric acid, and deionized water (DI) for 60 s where AZ 5412 photoresist was used to define the cantilevers. An AZ 5214 resist layer was then patterned and developed to protect the Si_3N_4 during the xenon difluoride (XeF_2) final dry-etch release, and to ensure that Si etching only occurred surrounding the devices to achieve the desired release of the cantilever actuator devices.

Fig. 2 Fabrication process for the NiTi cantilevers

2.4 Temperature-Dependent Bending of Released NiTi/Pt Cantilever Bimorph Actuators

To inspect the temperature-dependent equilibrium curvature of the NiTi on Pt MEMS cantilevers, we positioned the 7 mm x 7 mm device substrates on a 1-inch hotplate connected to and controlled by a Linkam TMS91 temperature control box. For this experiment, we gradually heated and cooled the sample chip at 3 °C/min, to match the rate of the wafer bow measurements taken for the stress versus temperature data. We used a Keyence VW-600C high-speed (color) tilting microscope to take an angled video of the equilibrium heating and cooling of the cantilevers, as depicted in Fig. 3. The Keyence microscope was attached to a Keyence VHX-1000 external monitor, which recorded and displayed the live-feed video. We used windows movie maker to post-process the videos for tasks such as speeding up playback and including a temperature display.

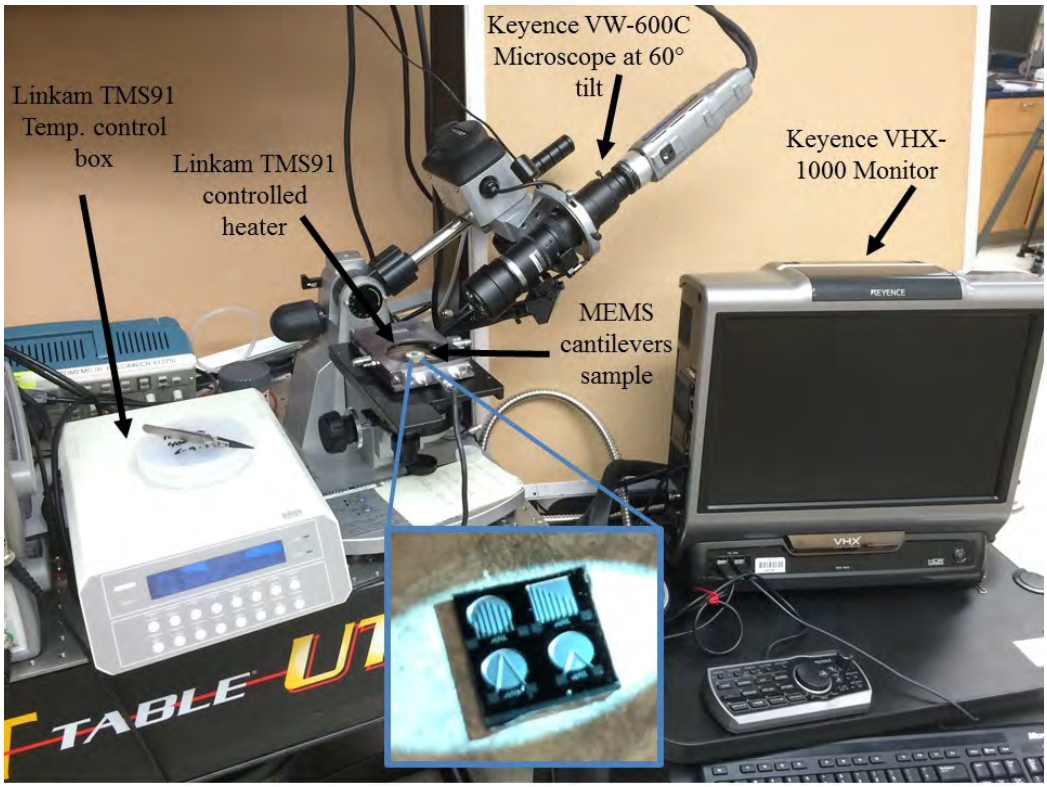

Fig. 3 Experimental setup for equilibrium heating and cooling experiment with a tilted Keyence microscope (Insert: typical 7 mm x 7 mm chip used for testing)

3. Results and Discussion

3.1 SEM Inspection of NiTi Films After Sputter Deposition

We sputtered different thicknesses of NiTi onto Si wafers using various sputter parameters. Additionally, we sputtered NiTi onto 200-nm Pt on Si to represent our cantilever bimorphs. Originally, we deposited the NiTi at RT and then annealed the samples at 600 °C for 1 h in order to crystalize the NiTi. We then sputtered the NiTi above its' crystallization temperature (~450 °C) at 600 °C and found that when sputtered at 600 °C the NiTi came out more uniform and with less cracks in the film, as shown in Fig. 4. Sputtering NiTi above ~450 °C, therefore, appears to result in crystallized films, which is necessary for the shape memory effect and eliminates the post-sputter crystallization step required otherwise.

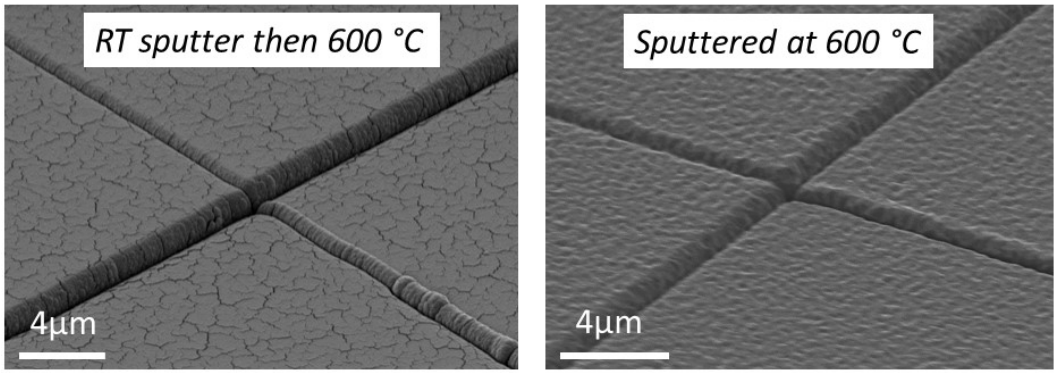

Fig. 4 Surface texture comparison between NiTi sputtered at RT, then annealed at 600 °C, and NiTi sputtered at 600 °C

We prepared samples of NiTi sputtered onto Si wafers, and NiTi on Pt in order to measure and calculate NiTi stress versus temperature under various sputtering conditions. As mentioned previously, one of the ways to achieve low residual stress and large recovery stress is to vary the NiTi sputtering parameters. We prepared 16 different samples, as shown in Table 1, each with varied Ar pressure, sputter temperature, anneal temperature, and thickness. The sample number corresponds to the specific NiTi-wafer. NiTi was sputtered onto Si for all wafers except where noted by *, meaning the NiTi layer was sputtered on a 200-nm Pt layer on a Si wafer. One sample with a bare layer of 200-nm Pt on Si wafer was used as a baseline to determine the temperature dependent stress of annealed Pt on Si.

Table 1 Sputter parameters used for NiTi on Si (100) wafers for stress vs. temperature measurements

Sample	Pressure (mTorr)	Sputter Temp (°C)	Anneal (°C)	Thickness (nm)
1	10	RT	600	1114
2	10	RT	600	906
3	10	RT	600	952
4	10	RT	600	2102
5	10	RT	600	2325
6	10	RT	600	2004
7	10	600	--	934
8	10	600	--	527
9	10	600	--	341
10	10	600	--	269
11	5	600	--	525
12	2	600	--	1607
13*	10	600	--	987
14*	10	600	--	981
15*	5	600	--	1126
16*	2	600	--	1651

3.2 Uniformity of the NiTi Co-Sputter Process

In order to test the uniformity of the NiTi after deposition, we performed a 4-point probe measurement on the surface of sample number 12. We measured the film resistivity at 25 points in a circular pattern around the wafer, from which we generated the contour plot of NiTi resistivity (Ω-cm) in Fig. 5. We calculated the uniformity of 93% for the sheet resistivity using

$$Uniformity = \left(1 - \frac{std}{mean}\right) * 100 \quad (3)$$

The discrepancy at the bottom of the wafer was due to masking off a region at the wafer flat, which we used to measure the NiTi film thickness using contact profilometry. Overall, these results suggest that our NiTi sputtering process is highly uniform across a 4-inch wafer, which gives us confidence that devices distributed anywhere across the wafer should behave with relative repeatability.

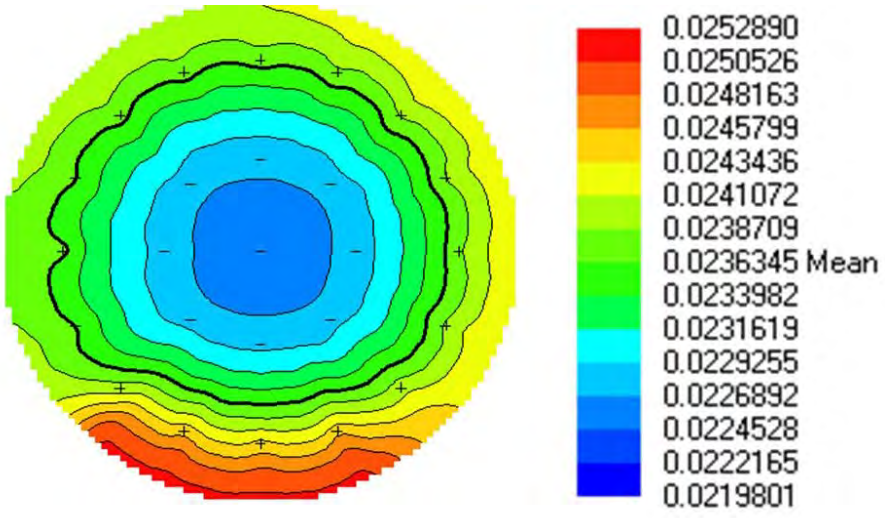

Fig. 5 Contour plot representing the uniformity of the NiTi deposited across a 4-inch wafer based on 25 surface resistivity measurements for the nominal 600 °C sputter-deposition of NiTi on Si (100) wafer

One difference that was noticed between the samples that were deposited at RT and the ones that were deposited at 600 °C was the temperature at which the supposed phase transition occurred. The phase transition occurred at a higher temperature when the NiTi was deposited at 600 °C compared to a RT deposition with 600 °C anneal. Generally the phase transition onset was at 60 °C for the 6 RT sputtered samples. Whereas the phase transition onset was between 65–75 °C for the samples sputtered at 600 °C. We performed EDX measurements to test if the NiTi deposited at 600 °C was still equiatomic, since the same nominal powers were used as in the RT sputter process resulting in equiatomic films. Using a FEI NanoSEM 600 with

EDAX detector, we discovered that the films had become Ti rich when using the nominal target powers and sputtering at 600 °C, as shown in Table 2. It is known from literature that a Ti-rich film can increase the temperature of the phase change.[6] Therefore, we attributed this subtle increase in temperature of the phase transition to the deposition of the NiTi at 600 °C, which consequently yielded a Ti-rich film. It may eventually be necessary to perform a study to determine the necessary target powers to use during the 600 °C deposition to achieve an equiatomic film of NiTi. This would be achieved by fixing the NiTi target power at its nominal value of 375 W and incrementally decreasing the Ti target power to determine the Ti power, which results in an equiatomic film of NiTi.

Table 2 EDX results for NiTi samples deposited at 600 °C, using the nominal target powers resulting in equiatomic films sputtered at RT

Sample	at %
10	$Ti_{57}Ni_{43}$
13	$Ti_{57}Ni_{43}$
14	$Ti_{56}Ni_{44}$
15	$Ti_{56}Ni_{44}$

3.3 Stress vs. Temperature Measurements for NiTi on Si and Si/Pt

We measured stress versus temperature while gradually heating the wafers starting from RT and up to 100 °C at a rate of 3 °C/min. The stress versus temperature plots for all the samples varied (Figs. 6–9). However, there were some characteristics shared by all of the NiTi samples and their respective stress versus temperature plots. Each of the samples had a phase change onset between 60 and 80 °C, whether the sample was deposited on Pt or Si. As stated above, the reason that samples 1–6 had lower phase change temperatures was due to the equiatomic NiTi film. For samples 7–16, the NiTi was approximately $Ti_{56}Ni_{44}$, and Ti-rich films translated to higher phase change temperatures.

The optimal situation is a NiTi cantilever with low residual stress, large recovery stress, and general repeatability. Our goal was to have a repeatable sample with relatively low residual stress and relatively large recovery stress. For the first 6 samples, we measured baseline residual stress as low as 330 MPa with recovery stresses of up to 62 MPa.

NiTi samples 7–12 were all deposited at 600 °C. There were noticeable differences from the first 6 samples in regards to stress versus temperature data. The 600 °C samples generally had lower residual stress, larger recovery stress, and were

completely reversible. Both graphs 8 and 11 show a completely reversible process that also shows the general characteristics of the NiTi shape memory alloy. For graphs 8 and 11, the hysteresis is as large as 75 °C, while for graph 9, the hysteresis is approximately 15 °C.

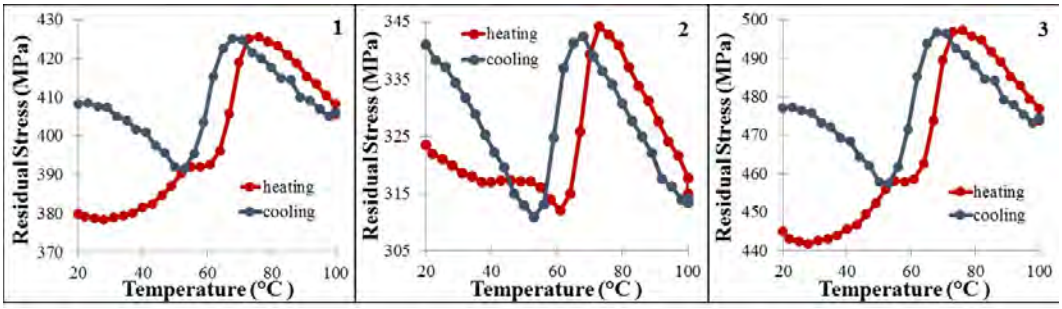

Fig. 6 Stress vs. temperature plots for samples 1–3, NiTi on Si

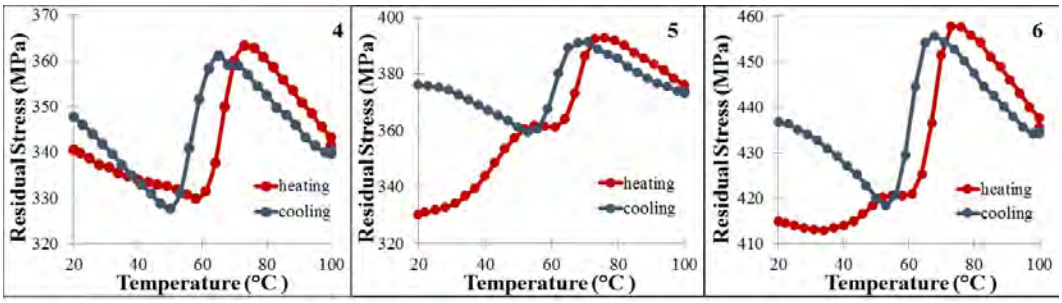

Fig. 7 Stress vs. temperature plots for samples 4–6, NiTi on Si

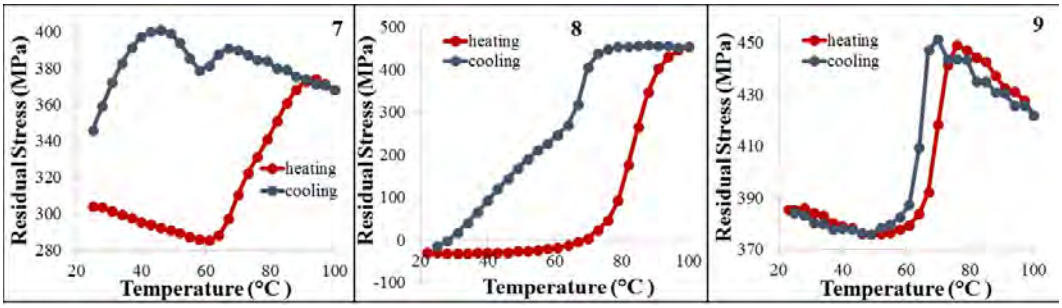

Fig. 8 Stress vs. temperature plots for samples 7–9, NiTi on Si

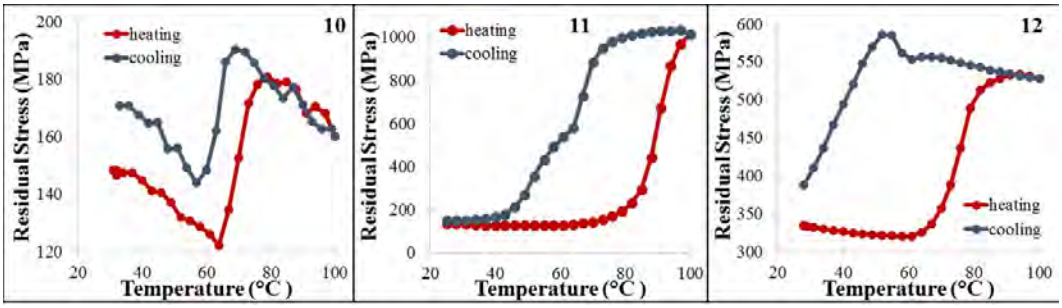

Fig. 9 Stress vs. temperature plots for samples 10–12, NiTi on Si

We deposited NiTi onto a layer of Pt for samples 13–16. We did this so the stress versus temperature data were representative of the NiTi cantilevers on Pt. We discovered that after annealing Pt at 600 °C for 1 h, the RT residual stress in Pt is ~2,200 MPa, as shown in Fig. 10. Causes for such large stresses could be large differences in thermal expansion of Si and Pt, the extremely large temperature gradient of nearly 600 °C, and alloying between Pt and Si. Therefore, there is a difference in the stress versus temperature data from the NiTi on Pt samples and the NiTi on Si samples. The RT residual stress from samples 13–16 are comparable to the NiTi on Si samples. The reason for this being, only the residual stress and recovery stresses for the NiTi was calculated in the NiTi-Pt bimorph. The 21 °C residual stress ranges from –86 to 363 MPa. In Fig. 11, sample 13 shows an interesting characteristic that is not present in any of the other samples. On cooling, after the drop in residual stress, it flattens out and remains constant for ~20 °C.

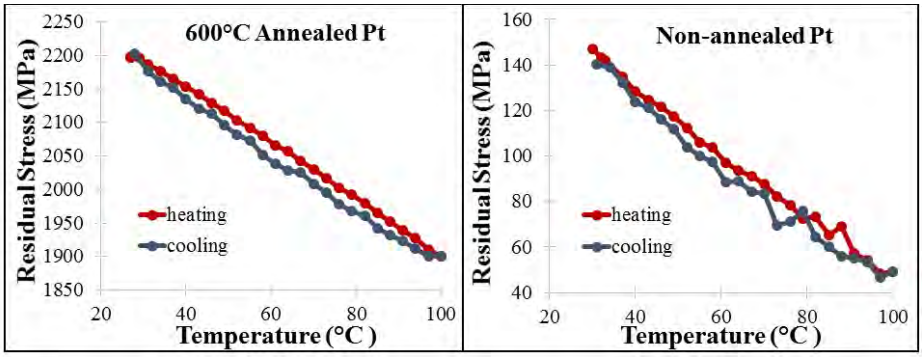

Fig. 10 Stress vs. temperature for annealed and non-annealed Pt

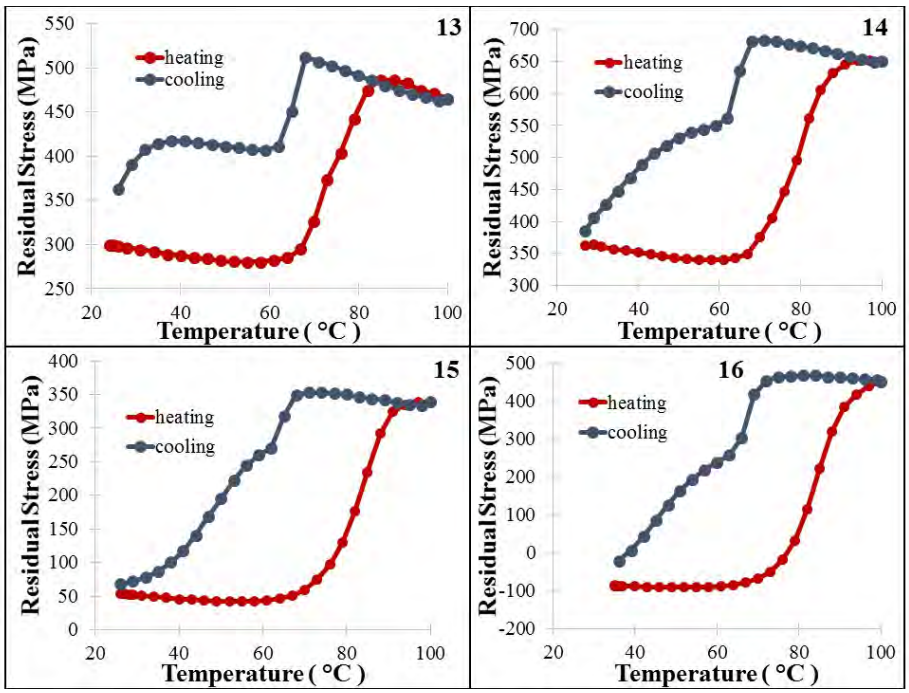

Fig. 11 Stress vs. temperature plots for samples 13–16, NiTi on Pt

Another important aspect when looking at the NiTi thermally actuated MEMS cantilevers is how quickly they returned to their original state, which is generally controlled by the hysteresis in the shape memory effect. A larger hysteresis simply means that the sample needs to be cooled over a larger temperature range, which would result in slower transformations. It is evident from these plots that for the first 6 samples, the cantilevers quickly returned back to their original position, due to the narrow hysteresis of nearly 3 °C. However, the residual stress spikes back up, leading to a non-repeatable phase change for samples 1–6, which were sputtered at 21 °C and then annealed at 600 °C. We note that hysteresis in the 600 °C samples could be as large as 40 °C, which is quite large when thinking about thermally cycling a device based on this material.

As mentioned previously, the goal was to achieve low RT residual stress with a large recovery stress. Figure 12 shows a summary of all the NiTi on Si samples. There are 2 samples that show these desired characteristics. Both samples 8 and 11 show relatively large recovery stress (up to 882 MPa) and relatively low RT residual stress (as low as –29 MPa). Both of these samples had a NiTi thickness of ~525 nm, which indicates that a 500-nm film of NiTi with exceptional shape memory properties can be achieved.

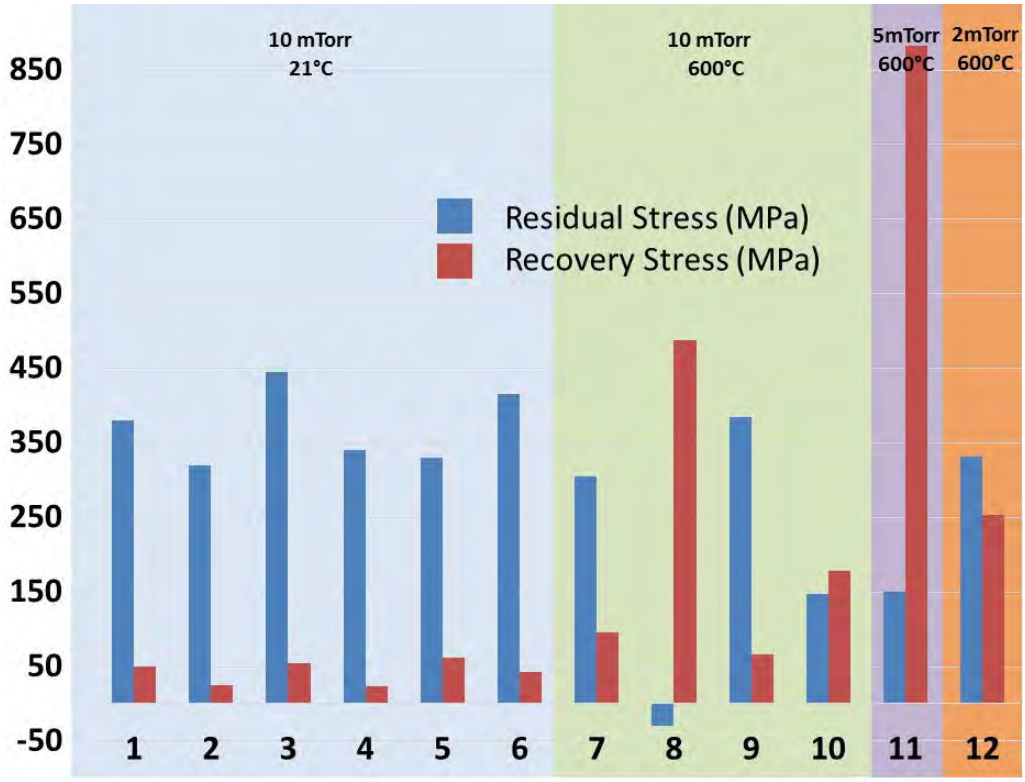

Fig. 10 Summary of residual and recovery stress for samples 1–12, all of which are NiTi on Si

Figure 13 is a summary of the RT residual stress, and recovery stress for samples 13–16, corresponding to NiTi on Pt. Even though samples 13 and 14 have the same parameters and similar thicknesses, they appear to be very different. Sample 13 came out of the AJA tool before it had completely cooled down, which is likely the cause for disagreement between the 2 samples. The differences in stress could be due to the fact that the film may have oxidized when it came out hot. This could account for the reduction in recovery stress, since oxidized NiTi is known to have diminished shape memory properties. The change in RT residual stress could be a result of the rapid cooling of sample 13.

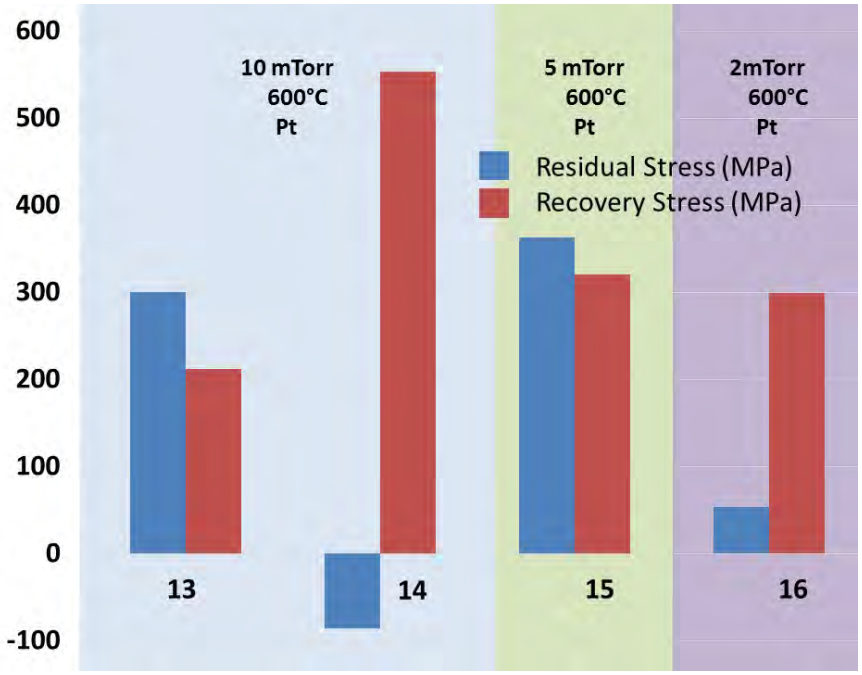

Fig. 11 Summary of residual and recovery stress for samples 13–16 all of which are NiTi on Pt

It is interesting to note that samples 8 and 14 are both very similar. Even though sample 8 had NiTi sputtered on Si and sample 14 had NiTi sputtered on Pt, they both have approximately –50 MPa RT residual stress, and approximately 550 MPa recovery stress. Both had the same sputtering parameters with only a difference of 450 nm NiTi. Not only are the residual stress and recovery stress similar, but also the shapes of the stress versus temperature plots.

3.4 Temperature-Dependent Bending of Released NiTi/Pt Cantilever Bimorph Actuators

In order to test the temperature-dependent behavior of the released cantilevers, we tested devices by slowly heating them at 3 °C/min from RT to 99 °C and cooling them at 3 °C/min back to RT. As shown in Fig. 14, the cantilevers curl and reach a

maximum displacement out of plane at 74 °C, and then rapidly fold flat until 99 °C. On cooling, the cantilevers remain flat, at which point they rapidly curl upward at 63 °C and remain curled until 37 °C where they begin to fall flat until RT. It was interesting to note that the degree of curvature (and thus out of plane displacement) was roughly constant over the 63 to 40 °C temperature window upon cooling, a behavior that was consistent with the stress plateau upon cooling for sample 13, which also corresponds to a NiTi/Pt/Si stack of 987-nm NiTi, 200-nm Pt. The devices we tested were made using the same sputter recipe as sample 13 and NiTi thickness was measured to be 1.4 µm using contact profilometry.

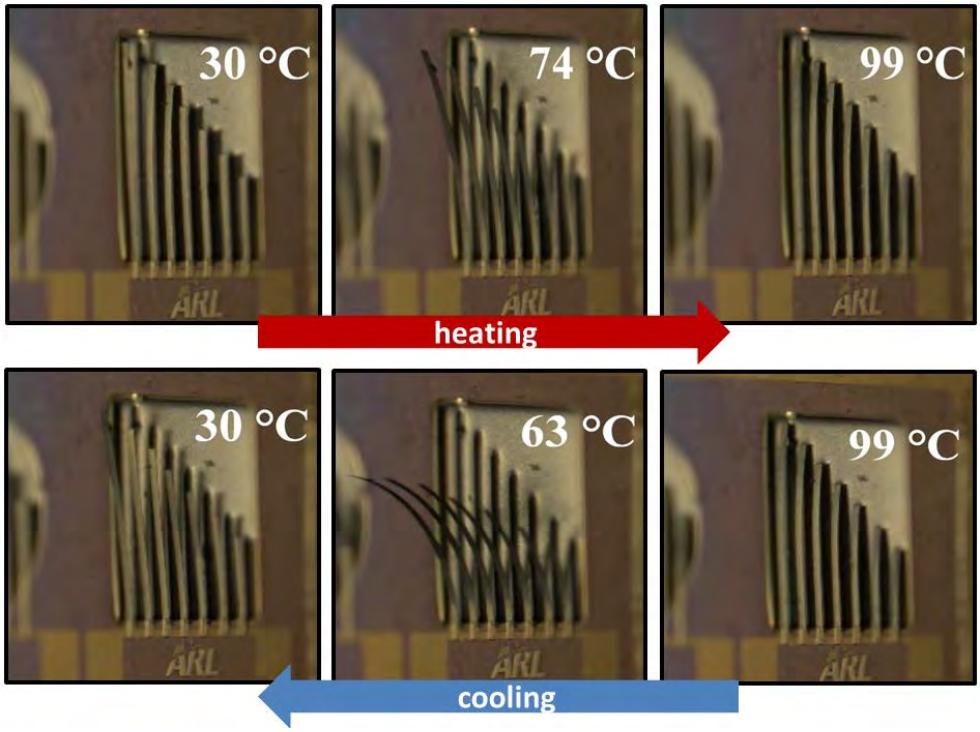

Fig. 12 Device testing at 3 °C/min from 30 to 99 °C and back to 30 °C

4. Conclusions

We have characterized sputter-deposited NiTi thin films, which are useful for creating NiTi thin-film cantilever actuators. We created 16 samples of NiTi on 4-inch Si wafers to test different deposition parameters, and try to make a useful cantilever with low RT residual stress and large recovery stress. We found after our first 6 samples, that rather than depositing the NiTi at RT and then annealing it at 600 °C for 1 h, a smoother film is created if the NiTi was deposited at 600 °C. After EDX tests, we found that while depositing at RT the NiTi was equiatomic, but when depositing NiTi at 600 °C, the films became Ti rich, which lead to a higher phase change temperature.

Through stress versus temperature data, we determined the deposition parameters that result in the most ideal film conditions based on residual and recovery stresses. From the stress versus temperature data, we can concluded that our 2 best samples are samples 8 and 11, both of which have 527 and 525 nm of NiTi, respectively. Through varying the deposition parameters, we improved the residual stress from ~400 MPa down to –29 MPa. We also improved the recovery stress from ~40 MPa up to 882 MPa.

We reported on our first basic demonstrations of thermally actuated cantilevers with intent to characterize these devices more extensively in future work.

5. References

1. Fernandes FMB, Martins R, Noguiera T, Silva RJC, Nunes P, Costa D, Ferreira I, Martins R. Structural charcterisation of NiTi thin film shape memory alloys. Sensors and Actuators A. 2002;99:55–58.

2. Ohta A, Bhansali S, Kishimoto I, Umeda A. Novel fabrication techique of TiNi shape memory alloy film using separate Ti and Ni targets. Sensors and Actuators. 2000;86:165–170.

3. Uchil J. Shape memory alloys - characterization techiques. Pramana - J. Phys. 2002;58:1131–1139.

4. Quandt E, Halene C, Holleck H, Feit K, Kohl M, Schloβmachera P, Skokana A, Skrobanckb KD. Sputter deposition of TiNi, TiNipd and TiPd films displaying the two-way shape-memory effect. Sensors and Actuators A. 1996;53:434–439.

5. Fu YQ, Luo JK, Hu M, Du HJ, Flewitt AJ, Milne WI. Micromirror structure actuated by TiNi shape memory thin films. J. Micromech. Microeng. 2005;15:1872–1877.

6. Sanjabi S, Cao YZ, Sadrnezhaad SK, Barber ZH. Binary and ternary NiTi-based shape memory films deposided by simultaneous sputter deposition from elemental targets. J. Vac. Sci. Technol. A. 2005;23:1425–1429.

7. Fu Y, Du H, Zhang S. Sputtering deposited TiNi films: relationship among processing, stress evolution and phase transformation behaviors. Surface and Coatings Technology. 2003;167:120–128.

8. Makino E, Mitsuya T, Shibata T. Micromachining of TiNi shape memory thin films for fabrication of micropump. Sensors and Actuators A. 2000;79:251–259.

9. Shih C-L, Lai B-K, Kahn H, Phillips SM, Heuer AH. A robust co-sputtering fabrication procedure for TiNi shape memory alloys for MEMS. J. MEMS. 2001;10(1):69–79.

10. Frantz-Rodriguez N, Bosseboeuf A, Dufour-Gergam E, Stambouli-Séné V, Nouet G, Seiler W, Lebrun J-L. Composition and structure of NiTiCu shape memory thin films. J. Micromech. Microeng. 2000;10:147–151.

11. Fu Y, Huang W, Du H, Huang X, Tan J, Gao X. Characterization of TiNi shape-memory alloy thin films for MEMS applications. Surface Coatings and Technology. 2001;145:1007–112.

12. Wibowo E, Kwok CY. Fabrication and characterization of sputtered NiTi shape memory thin films. J. Micromech. Mircroeng. 2006;16:101–108.

13. Grummon DS, Zhang J, Pence TJ. Relaxation and recovery of extrinsic stress in sputtered titanium-nickel thin films on (100)-Si. Materials Science and Engineering A. 1999;722–726.

14. Isalgue A, Seguin J-L, Bendahan M, Amigo JM, Esteve-Cano V. Shape memory NiTi thin films deposited at low temperature. Materials Science and Engineering A. 1999;717–721.

15. Ishida A, Sato M, Miyazaki S. Mechanical properties of Ti-Ni shape memory thin films formed by sputtering. Materials Scoemce and Engineering A. 1999;754–757.

16. Kahn H, Huff MA, Heuer AH. The TiNi shape-memory alloy and its applications for MEMS. J. Micromech. Microeng. 1998;8:213–221.

17. Knick CR, Morris CJ. Development and verification of sputtered thin-film nickel-titanium (NiTi) shape memory alloy (SMA). Adelphi (MD): Army Research Laboratory (US); July 2015. Report No.: ARL-TR-7364.

18. Knick CR, Morris CJ. Microfabricated cantilevers based on sputtered thin-film Ni50Ti50 shape memory alloy (SMA). Adelphi (MD): Army Research Laboratory (US); July 2015. Report No.: ARL-TR-7381.

19. Knick CR, Morris CJ. Material and process development of thin film shape memory alloy for MEMS actuator. In proceedings of the ASME Conference on Smart Materials, Adaptive Structures, and Intelligent Systems (SMASIS), Denver, CO, 2015.

List of Symbols, Abbreviations, and Acronyms

Ar	argon
Au	gold
Cr	chromium
DI	deionized water
EDX	energy-dispersive x-ray
HF	hydrogen fluoride
MEMS	microelectromechanical system
NiTi	nickel-titanium
NiTiCu	nickel-titanium-copper
Pt	platinum
RF	radio frequency
RT	room temperature
SEM	scanning electron microscope
Si	silicon
Si_3N_4	silicon nitride
SMA	shape memory alloy
XeF_2	xenon difluoride

1 (PDF) DEFENSE TECHNICAL INFORMATION CTR DTIC OCA

2 (PDF) DIRECTOR US ARMY RESEARCH LAB RDRL CIO LL IMAL HRA MAIL & RECORDS MGMT

1 (PDF) GOVT PRINTG OFC A MALHOTRA

3 (PDF) DIRECTOR US ARMY RESEARCH LAB RDRL SER L C KNICK C MORRIS B PIEKARSKI

INTENTIONALLY LEFT BLANK.